AIAA 2001–2463

Design of Low Reynolds Number Airfoils with Trips

Ashok Gopalarathnam,
Department of Mechanical and Aerospace Engineering
North Carolina State University
Raleigh, North Carolina 27695
Benjamin A. Broughton, Bryan D. McGranahan, and
Michael S. Selig
Department of Aeronautical and Astronautical Engineering
University of Illinois at Urbana-Champaign
Urbana, Illinois 61801

19th AIAA Applied Aerodynamics Conference
June 11–14, 2001/Anaheim, CA

Design of Low Reynolds Number Airfoils with Trips

Ashok Gopalarathnam,*
Department of Mechanical and Aerospace Engineering
North Carolina State University
Raleigh, North Carolina 27695

Benjamin A. Broughton,† Bryan D. McGranahan,‡ and Michael S. Selig§
Department of Aeronautical and Astronautical Engineering
University of Illinois at Urbana-Champaign
Urbana, Illinois 61801

A design philosophy is presented for low Reynolds number airfoils that judiciously combines the tailoring of the airfoil pressure distribution using a transition ramp with the use of boundary-layer trips. Three airfoils with systematic changes to the shape of the transition ramp have been designed to study the effect of trips on the airfoil performance. The airfoils were wind-tunnel tested with various trip locations and at Reynolds numbers of 100,000 and 300,000 to assess the effectiveness of the design philosophy. The results show that the design philosophy was successfully used in integrating a boundary-layer trip from the outset in the airfoil design process. At the Reynolds numbers and the range of airfoil shapes considered, however, airfoils designed with trips do not hold any clear advantage over airfoils designed for good performance in the clean condition.

Introduction

IT is well known that for an airfoil to achieve low drag in a low Reynolds number (60,000 $< Re <$ 500,000) environment, it is important to eliminate or reduce the drag caused by the laminar separation bubble, referred to here as "bubble drag." One of the ways of reducing the bubble drag is by the use of a transition ramp,[1–3] which is the long region of adverse pressure gradient used to destabilize the laminar boundary layer and promote transition while avoiding large transitional bubbles. The shape of the transition ramp is also closely associated with the variation of the chordwise transition location x_{tr}/c with lift coefficient C_l. The larger the change in the x_{tr}/c for a given change in C_l, the lower is the bubble drag. Although a shallower transition curve results in lower bubble drag, it also results in a smaller C_l range over which this low drag can be achieved. Thus, the designer has to make a trade-off between a decrease in the bubble drag and the C_l range over which this low drag is achieved.[3]

A second means of reducing bubble drag is by the use of boundary-layer trips to completely eliminate or at least reduce the intensity of the laminar bubble. Trips are often used to "repair" the performance of an airfoil that has a large bubble drag in the clean configuration.

The objective of the current work is to develop a philosophy for the design of low Reynolds number airfoils that integrates the use of trips from the beginning in the airfoil design process. The key idea is to judiciously combine the use of a transition ramp to achieve low bubble drag over one portion of the drag polar and to use boundary-layer trips to extend the C_l-range over which low bubble drag is obtained. A primary aim of the work is to determine whether an airfoil designed to use trips will have a better performance overall than one designed for good performance when clean.

The following section briefly describes the two common approaches to achieving low bubble drag, namely the use of (1) transition ramps and (2) boundary-layer trips. The design philosophy developed in the current work to integrate trips in the airfoil design process is then described. Experimental results are then presented to demonstrate the effectiveness of the design philosophy. Results for three airfoils are presented both with and without boundary-layer trips on the upper surface. The three airfoils have been designed with systematic changes to the shape of the transition ramp

*Assistant Professor, Box 7910. e-mail: ashok_g@ncsu.edu Member AIAA.

†Graduate Research Assistant, 306 Talbot Laboratory, 104 S. Wright St. e-mail: bbrought@uiuc.edu. Student Member AIAA.

‡Graduate Research Assistant, 306 Talbot Laboratory, 104 S. Wright St. e-mail: mcgranah@uiuc.edu. Student Member AIAA.

§Associate Professor, 306 Talbot Laboratory, 104 S. Wright St. e-mail: m-selig@uiuc.edu. Senior Member AIAA.

with the specific objective of studying trip effects.

Means of Achieving Low Bubble Drag

As described earlier, there are two common means used to achieve low bubble drag on airfoils operating at low Reynolds numbers: (1) by tailoring the transition curve (transition ramp), or (2) by use of boundary layer trips. In this section, these two methods will be examined briefly to understand how they affect the size of the bubble and the resulting drag.

Effect of the transition curve on drag

The effect of the transition curve is demonstrated[4] using two example airfoils A and B. Figure 1 shows a comparison of the geometries and inviscid velocity distributions for the two airfoils. These airfoils were designed using PROFOIL,[5,6] a multipoint inverse airfoil design method based on conformal mapping. The two airfoils were designed to have two different shapes for the transition ramp on the upper surface. The airfoils were then analyzed using XFOIL,[7] and Fig. 2 shows the drag polars and upper-surface transition curves for a Reynolds number of 200,000. For the sake of this discussion, the transition ramp is defined here as the region over which the bubble moves gradually as defined by the transition curve.

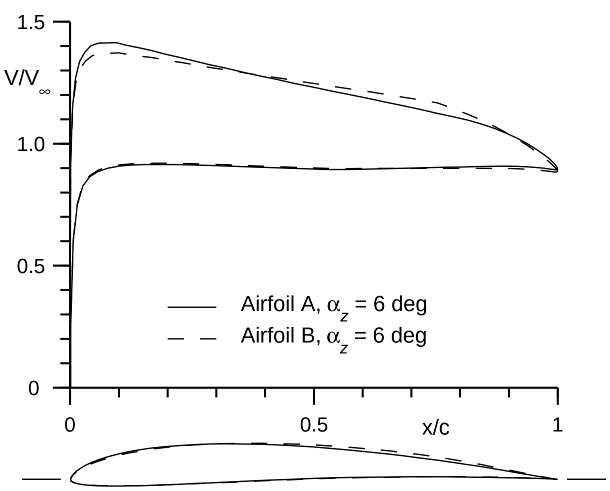

Fig. 1 Inviscid velocity distributions for airfoils A and B to study the different effects on drag.

From Fig. 2, it can be seen that airfoil A has lower drag than airfoil B at lift coefficients from around 0.3 to around 0.7, above which airfoil B has lower drag. Also noticeable is the correlation between the drag polar and the shape of the upper-surface transition curve. For the C_l-range from 0.3–0.7, where airfoil A has lower drag, the transition curve for airfoil A is shallower than for airfoil B. That is, there is a larger change in the value of x_{tr} for airfoil A than for B. For values of C_l from 0.7–1.2 where airfoil B has lower drag, the transition curve for airfoil B is shallower than for A. This figure shows that the steepness of the transition curve is a direct indication of the bubble drag. By adjusting the shape of this curve, it is possible to tailor the drag polar of an airfoil at low Reynolds numbers.

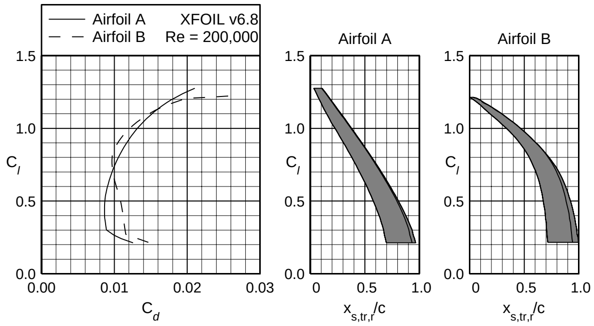

Fig. 2 XFOIL predictions for airfoils A and B to illustrate the effects of changes in the transition ramp on drag.

Figure 2 also includes an overlay of the variation of bubble size $(x_r - x_s)$ with C_l. The size of the bubble for each C_l was obtained by determining the chordwise extent over which the skin-friction C_f, as predicted by XFOIL, was less than or equal to zero. Studying the bubble-size variation for the two airfoils further illustrates the connection between the shape of the transition curve and the bubble drag. The bubble is larger when the transition curve is steeper.

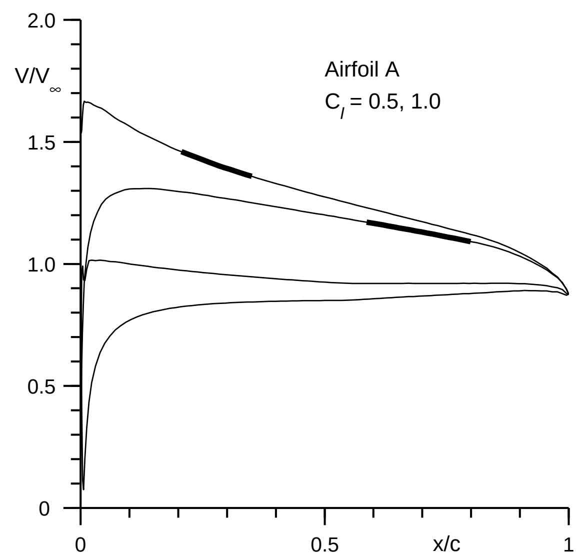

Fig. 3 Inviscid velocity distributions for airfoil A with the locations of the bubble marked.

Figure 3 shows the inviscid velocity distributions for airfoil A at C_l values of 0.5 and 1.0 with the upper-surface bubble location marked in bold. A similar plot for airfoil B is shown in Fig. 4. Comparing the velocity

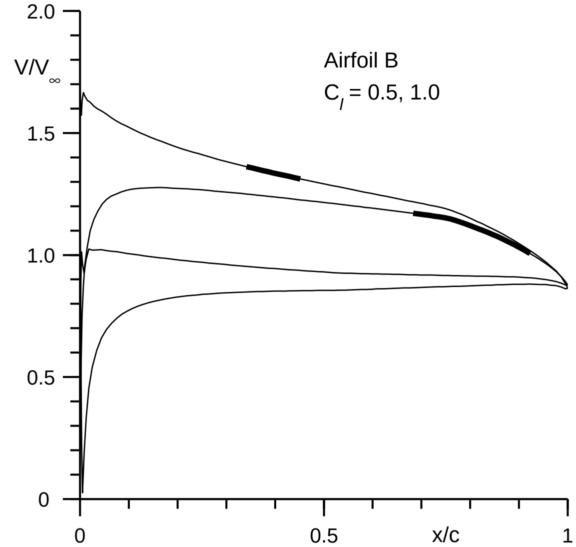

Fig. 4 Inviscid velocity distributions for airfoil B with the locations of the bubble marked.

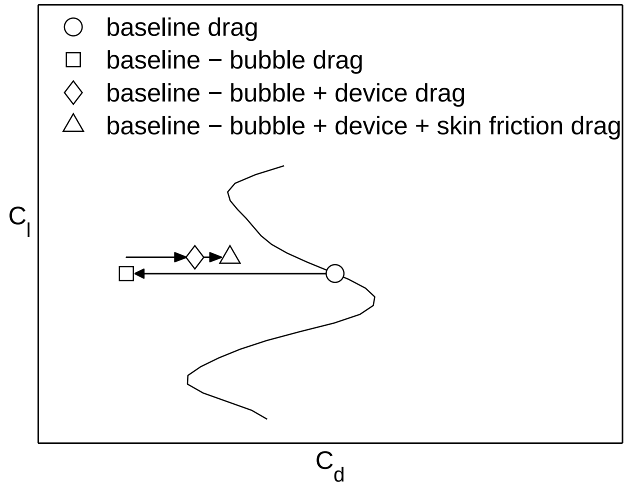

Fig. 5 Conceptual illustration of trip effects.[8,9]

drops across the bubble for the four cases, it can be seen that while airfoil A has a smaller velocity drop than airfoil B at $C_l = 0.5$, the situation is reversed for $C_l = 1.0$. Since the pressure drag due to the bubble increases with increasing velocity drop across the bubble, airfoil A has smaller bubble drag at the low C_l and larger bubble drag at the higher C_l. Thus, a steeper transition curve results in a larger bubble and also larger velocity drop across the bubble causing an increase in bubble drag.

Effect of the trips on drag

Trips have been widely used[1,8–12] to improve performance of airfoils having high bubble drag. As described in Refs. 8 and 9, trips (when properly designed) can cause a net reduction in the drag as a consequence of three main effects: added device drag, a reduction in bubble drag and an increase in skin-friction drag. Figure 5, taken from Refs. 8 and 9, shows how the cumulative result of these three effects can reduce the overall drag at a particular C_l. Figure 6, shows an example where the use of trips has resulted in significant drag reductions for an airfoil having large bubble drag.

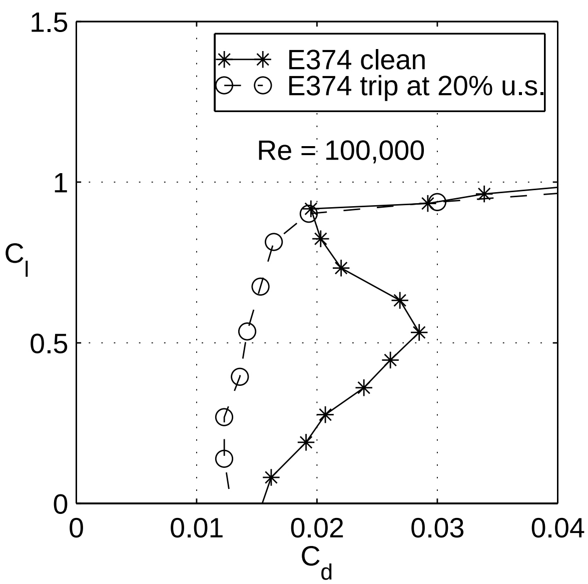

Fig. 6 Effect of a trip on the E374 polar at $Re = 100,000$ (data from Ref. 10).

Design Philosophy for Airfoils with Trips

To illustrate the philosophy for designing airfoils to use trips from the outset to achieve good performance, the two airfoils A and B from the preceding section are reconsidered. As seen from Fig. 2, airfoil B has lower drag at the higher C_l values and has higher drag at the lower C_l values. As discussed earlier, the higher drag for B at the lower C_l values is associated with the steeper transition curve for this airfoil at these C_l values. A question can now be posed: Would it be possible to extend the low-drag behavior of airfoil B at high C_l values to lower C_l conditions by using a boundary-layer trip upstream of the bubble to reduce the intensity of the bubble at the lower values of C_l, and would such a trip configuration result in a performance that is better overall than that of airfoil A?

To explore this option in greater depth, XFOIL was used to study the effect of fixing the upper-surface transition location on airfoil B. Figure 7 compares the resulting drag polar with those for the clean airfoils A and B. As seen from the figure, the performance of airfoil B with transition fixed at 65% on the upper surface is superior to those of the clean airfoils A and B. It must be remembered, however, that when analyzing an airfoil using XFOIL with fixed transition at a specified location, XFOIL assumes instantaneous

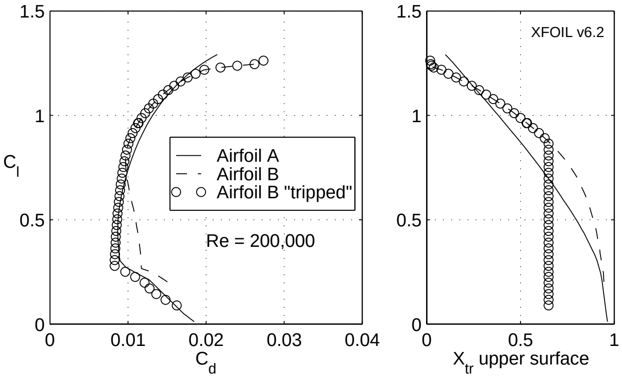

Fig. 7 Effect of fixing transition on the upper surface of airfoil B, as predicted by XFOIL.

transition from laminar to turbulent flow at that point and results in complete elimination of any bubble that might have otherwise occurred downstream of that point. In reality, however, the disturbance resulting from trips on low Reynolds number airfoils do not cause instantaneous transition at the trip location. As the experimental results of Ref. 8 show, trips on airfoils at low Reynolds numbers need to be located several tenths of chord upstream of a bubble to significantly diminish the bubble intensity. Many trip configurations are also unsuccessful in completely eliminating the bubble. Also no device drag is assumed in the XFOIL when fixing transition.

In spite of the limitations of XFOIL in accurately modeling boundary layer trips, the results in Fig. 7 do provide confidence that a judicious combination of the transition ramp and a boundary-layer trip can result in an airfoil having a better performance overall than one designed for good performance when clean. More specifically, an airfoil designed for use with trips will need to have the transition ramp tailored so that it results in low drag at the higher values of C_l with a shallow slope for the transition curve at these values of C_l. At lower values of transition curve needs to have a steeper slope which results in a larger bubble drag. The boundary layer trip, located on the upper surface at a forward location can be used to diminish the bubble at low values of C_l and "extend" the low drag achieved at the high values of C_l. Owing to the fact that there are no readily available computer programs that can accurately predict the effect of trips, experimental studies need to be made to determine the optimum trip location as well as the effectiveness of the design philosophy.

Experimental Investigation

In an effort to better understand the trade-offs involved in designing airfoils that judiciously combine the effect of the transition ramp and a boundary-layer trip, three airfoils were designed with systematically varying transition ramps on the upper surfaces. Figure 8 shows the three airfoils SA7024, SA7025, and SA7026 and inviscid velocity distributions at a C_l of 0.6. Figures 9 and 10 show the predicted performance for the three airfoils at Reynolds numbers of 100,000 and 300,000. The systematic variations in the transition ramps (i.e., shapes of the x_{tr}/c curves) for the three airfoils are clearly seen. One of the design objectives was that the extents of the low-drag ranges of these airfoil should be similar. For this objective to be satisfied in combination with the fact that the three airfoils had different transition-ramp shapes, it was necessary to design the three airfoils to have three different thicknesses. As a result, the SA7024, SA7025 and the SA7026 have a maximum thicknesses of 7%, 8%, and 9% respectively.

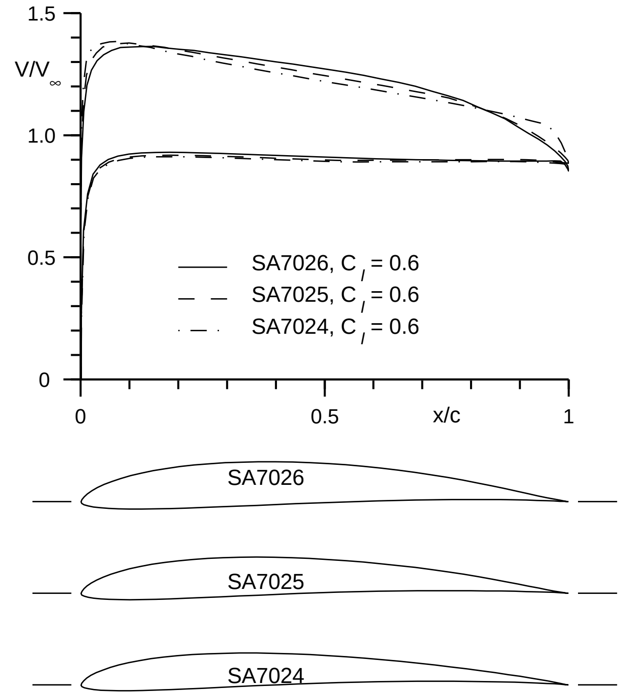

Fig. 8 SA702x airfoils and inviscid velocity distributions.

All experiments were performed in the UIUC open-return subsonic wind tunnel, more details of which are available in Refs. 9, 11, and 12. The lift was measured with a strain gage force balance rig. The drag was obtained from the momentum-deficit method. To ensure that the wake had relaxed to tunnel static pressure, the wake measurements were performed 14.8 in. (approximately 1.25 chord lengths) downstream of the trailing edge of the airfoil. Each vertical wake traverse consisted of between 20 and 80 total-head pressure measurements (depending on wake thickness) with points nominally spaced 0.08 in apart.

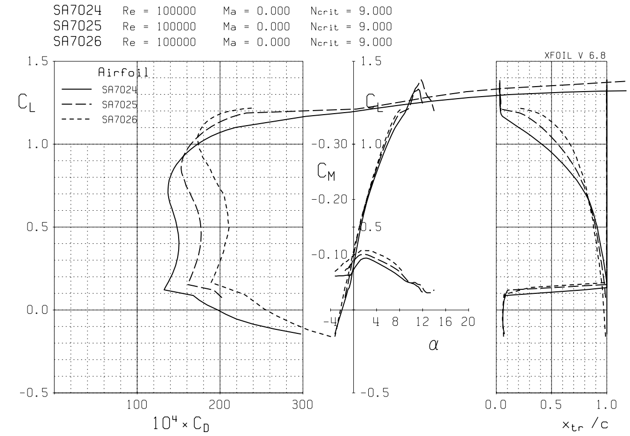

Fig. 9 XFOIL predictions for the SA702x airfoil series at Re of 100,000.

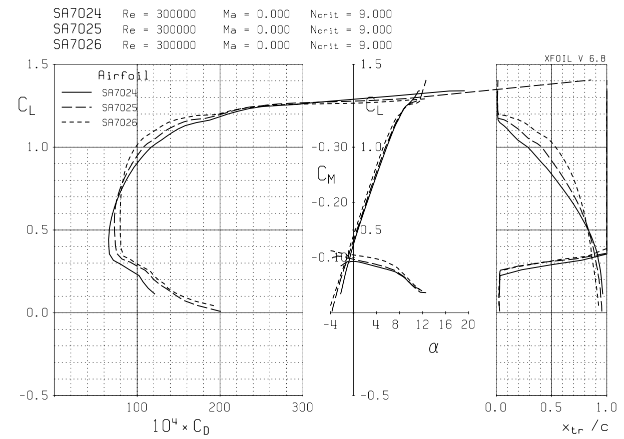

Fig. 10 XFOIL predictions for the SA702x airfoil series at Re of 300,000.

Experimental results

In this paper, the experimental results are presented for the airfoils SA7024, SA7025, and SA7026 at the Reynolds numbers of 100,000 and 300,000 and for four conditions: clean, trip at $0.1c$, trip at $0.2c$, trip at $0.3c$, and trip at $0.4c$.

All of the boundary-layer trips used in this study were constructed by using multiple layers of pressure-sensitive graphic tape, resulting in a total thickness of 0.0135 in. and a width of 1/8 in. They were placed on the airfoil such that the aft end of the tape was at the specified x/c location on the upper surface. In all cases, the trips used were placed on the upper surfaces of the airfoil, and the lower surface was left clean.

In this section, the experimental results for three airfoils in the clean condition are first presented. These results serve to compare experimental data with the XFOIL predictions. Next a matrix of drag polars are presented for the three airfoils and the four trip locations. In each polar plot, the drag polars for that airfoil and trip location at Re = 100,000 and Re = 300,000 are compared with the polars for the same airfoil in the clean condition at these Reynolds numbers. This matrix of polars allows comparison of drag for a given airfoil and different trip locations as well as for a given trip location for the three different airfoils. The last subsection then presents a comparison of the performance between the clean SA7024 and the tripped SA7026 in order to assess the design philosophy of designing an airfoil optimized for tripped performance to outperform an airfoil optimized for clean performance.

Additional crossplots comparing the lift and drag data for the three airfoils at different trip locations and Reynolds numbers are presented in Appendix A. In Appendix B, lift and drag data for each airfoil are compared for different trip locations and different Reynolds numbers. Although the crossplotting of the results leads to a certain degree of repetition, it allows easy examination of trip effects and airfoil-change effects at the two Reynolds numbers, and it provides insight into the various trends that could be useful for designers and users of low Reynolds number airfoils. In addition, the results can also be used by researchers in developing empirical, theoretical and computational models to simulate the effects of boundary-layer trips on airfoils. Tabulated data is available upon request.

Results with no trip

Figures 11 and 12 show the experimental results for the three airfoils at Re= 100,000 and Re=300,000. Comparing the results in these figures with the XFOIL predictions in Figs. 9 and 10, it is clear that the trends between the predictions compare well with those seen in the experiments. It is also seen that the design objectives have been satisfied. Comparison of the results at Re = 100,000 between the predictions and the experiments show that XFOIL predicts lower drag in the portions of the polars where bubble drag is dominant. In the present study, however, the XFOIL code has been primarily used as an analysis tool to design airfoils with systematic variations in performance, and not necessarily in accurately predicting the absolute performance of each airfoil.

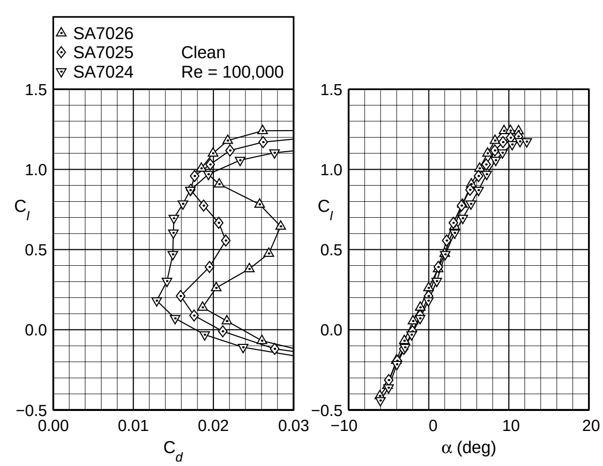

Fig. 11 Clean drag polars for Re = 100,000.

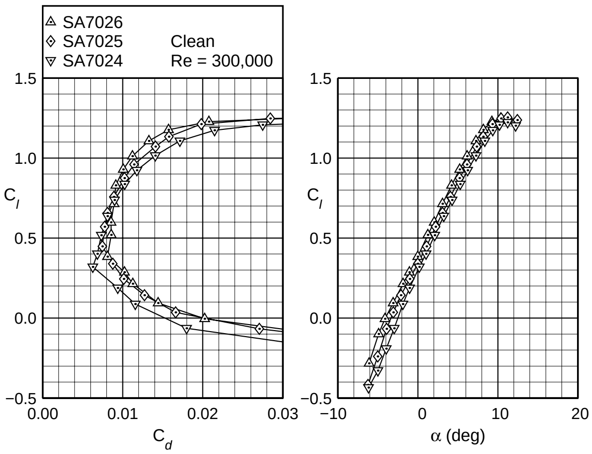

Fig. 12 Clean drag polars for Re = 300,000.

Comparison of drag polars

Figures 13–15 show the comparison of the tripped-airfoil performance with that of the clean airfoil for Re = 100,000 and Re = 300,000 for the three SA702x airfoils. All four trip locations have been considered.

Comparison of the tripped-airfoil polars for the SA7024 in Fig. 13a–d for Re = 100,000 shows that all the four trip locations are in general equally effective at reducing the bubble drag as compared with the clean case. At C_l=0.4, the 0.3c and 0.4c trip locations results in an approximately 0.002 greater reduction in C_d as compared with the more forward trip locations. At the higher Reynolds number of 300,000, there is clear increase in C_d for the 0.1c and 0.2c cases relative to the clean airfoil at C_l around 0.75. This increase in drag decreases progressively with aft movement of the trip location, and can be attributed to increasing amounts of laminar flow with the aftward movement of the trip location. The optimum location of the trip for the SA7024 airfoil is at 0.4c. At this location, there is a reduction in drag around C_l of 0.4 at Re = 100,000. Although there is small increase in C_d around C_l=0.1 at Re = 100,000, the airfoil on an airplane wing operates at higher Reynolds numbers at lower C_l values, and hence it may be expected that at C_l=0.1, the operating Reynolds number will be closer to 300,000.

As seen from Fig. 14a–d, for the SA7025 airfoil, trips at all the four locations reduce the C_d at Re = 100,000 over the range of C_l values where there is significant bubble drag. However, the magnitude of drag reduction at any particular C_l within this range depends on the location of the boundary-layer trip. At C_l values around 0.3, aft trip locations results in larger drag reduction owing to increased laminar flow. At C_l of around 0.8, the bubble has moved forward to around 0.4c. At this condition, the aft trip locations become less effective in reducing the drag particularly when the laminar separation location is upstream of the trip. A more forward location of the trip is therefore more effective at C_l of 0.8. In contrast, for the Re = 300,000 case, where bubble drag is less dominant, the forward trip locations result in higher drag around C_l of 0.8 owing to greater loss in laminar flow. All of the trip locations show a reduction in C_d of approximately 0.001–0.002 over the clean airfoil case at Re = 300,000 and C_l in the range of 0 to 0.4. Examination of the results shows that the 0.4c trip location appears to be the most beneficial. At this trip location, there is a modest reduction in the bubble drag at Re = 100,000, along with a reduction in C_d at the low C_l values and the higher Reynolds number. In particular, at this trip location there is no degradation in performance when compared with that of the clean airfoil.

The effect of different trip locations on the SA7026 airfoil, shown in Fig. 15a–d, is similar to that on the SA7025. At a C_l of around 0.4, the aft trip locations result in higher drag reductions at Re = 100,000 due to greater laminar flow when compared with the more forward trip locations. At C_l values in the vicinity of 0.8, the forward trip locations result in greater bubble drag reductions for Re = 100,000 because the trip is more upstream of the bubble. At the higher Reynolds number of 300,000, the forward trip locations result in an increase in the drag when compared with the clean airfoil because of increased skin friction resulting from loss in laminar flow. At the higher Reynolds numbers and lower C_l values of around 0.2, all of the trip locations result in a reduction in the drag over the clean airfoil. The optimum trip location for the SA7026 seems to be at 0.2c.

Comparison of the tripped SA7026 with the clean SA7024

In this subsection, a comparison of lift and drag data is presented in order to assess whether or not it is possible to design a low Reynolds number airfoil with a trip to have overall better performance than an airfoil designed for good performance when clean. For this purpose, the SA7024 airfoil is taken as an example of an airfoil designed for good performance when clean. The performance of the clean SA7024 is compared with that of the tripped SA7026 in Fig. 16. Although the SA7026 has poor performance in the clean condition, the 0.2c trip location significantly improves the overall performance of this airfoil. These results, therefore, serve as good examples of airfoils designed for good performance in the tripped condition using the design philosophy described in the previous section.

In making the assessment, the differences in performance at the lower C_l are studied at the higher Reynolds number of 300,000, while the differences in the polars at the higher C_l are evaluated at the lower Reynolds number of 100,000. Such as comparison is necessary for a wing airfoil as it takes into account the change in Reynolds number due to changes in flight speed of an airplane in rectilinear flight.

Comparison of the polars in Fig. 16 shows that the

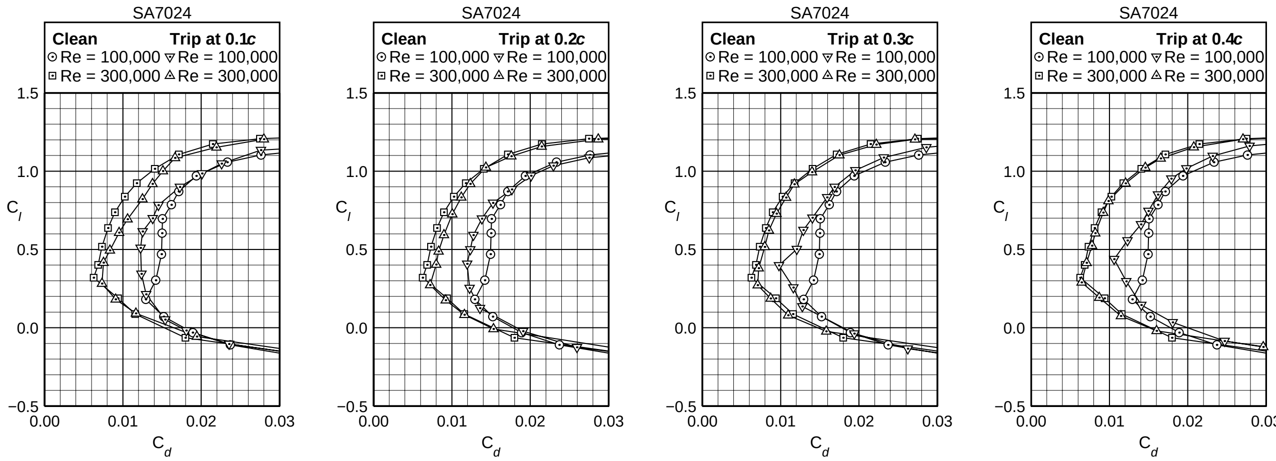

a) **Trip at 0.1*c*.** b) **Trip at 0.2*c*.** c) **Trip at 0.3*c*.** d) **Trip at 0.4*c*.**

Fig. 13 SA7024.

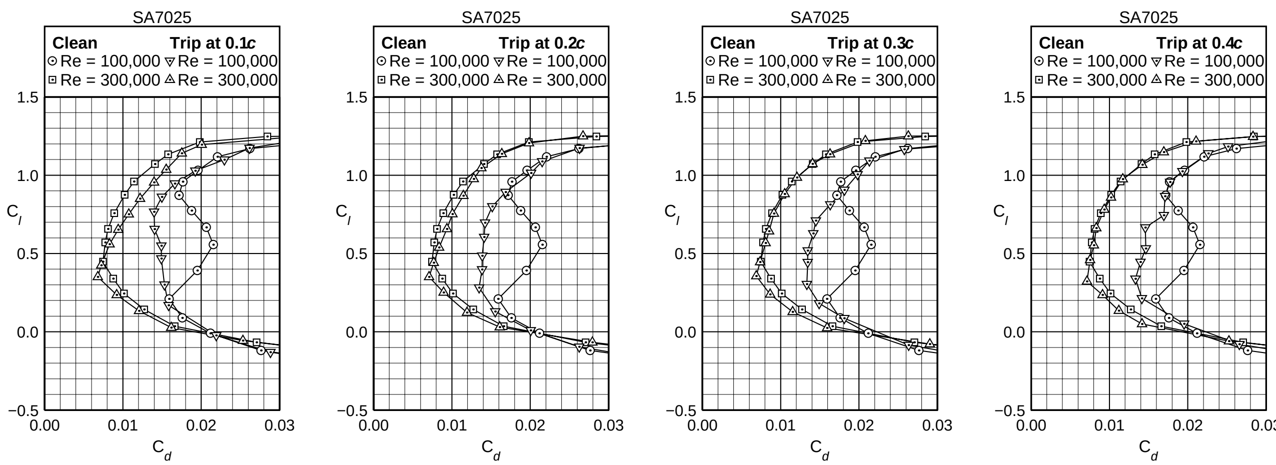

a) **Trip at 0.1*c*.** b) **Trip at 0.2*c*.** c) **Trip at 0.3*c*.** d) **Trip at 0.4*c*.**

Fig. 14 SA7025.

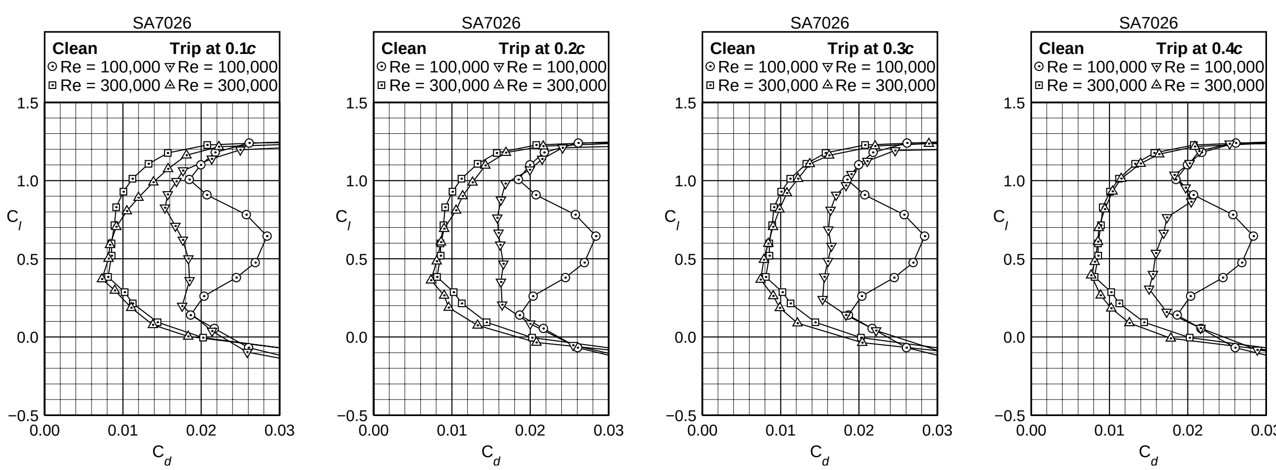

a) **Trip at 0.1*c*.** b) **Trip at 0.2*c*.** c) **Trip at 0.3*c*.** d) **Trip at 0.4*c*.**

Fig. 15 SA7026.

tripped SA7026 airfoil has a noticeably better performance than the clean SA7024 at $Re = 100{,}000$ and C_l values of around 1.0. At the low C_l values of around 0.3, however, the tripped SA7026 has higher drag than the clean SA7024 at $Re = 300{,}000$. This shows that for the range of Reynolds numbers and airfoil shapes considered in this study, the design philosophy described in the previous section has not resulted in a tripped airfoil with an uncompromised improvement over a clean airfoil at all flight conditions. The tripped airfoil does show an improvement at the high-C_l, lower Reynolds number condition, but this improvement is compromised by a small, but important loss in performance at the low-C_l, higher Reynolds number condition.

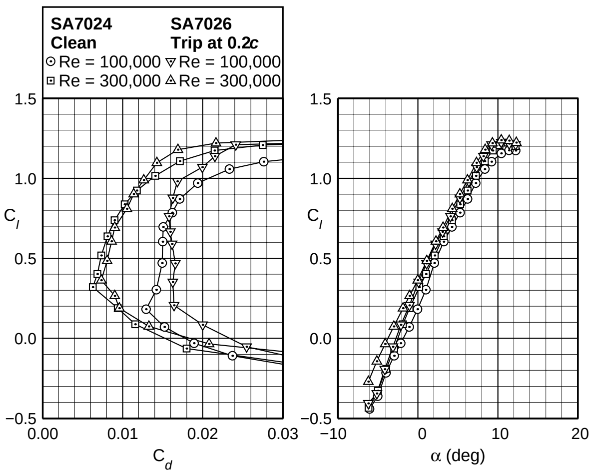

Fig. 16 Comparison of the 0.2c-tripped SA7026 with the clean SA7024.

Conclusions

A study has been presented to assess whether it is possible to design low Reynolds number airfoils to make judicious use of both transition ramps and boundary-layer trips in order to achieve a better performance overall when compared to an airfoil designed for the clean condition. A design philosophy has been presented for designing low Reynolds number airfoils to have good performance in the tripped conditon. For this study, a series of three airfoils were designed with systematic changes to the shape of the transition ramp. The three airfoils were wind-tunnel tested at Re = 100,000 and Re = 300,000 and at four conditions: clean, and with the trip located at 0.1c, 0.2c, 0.3c, and 0.4c.

An analysis of the results shows that for the Reynolds number range and the airfoils considered in this study, the airfoil optimized for the tripped condition has lower drag at the high-C_l, lower Reynolds number condition when compared with the airfoil optimized for clean performance. But this improvement is compromised by a small, but noticeable loss in performance at the low-C_l, higher Reynolds number condition. Tripped airfoil may also prove to be advantageous for design situations that need thicker airfoils or where the operating Reynolds numbers are less than 100,000. Additionally, this study also confirms the perhaps well-known fact that for a given airfoil, a single trip location is not the optimum for different flight conditions. Finally the study highlights the needs for empirical and computational models that can account for the different effects of boundary-layer trips during the design stages of a low Reynolds number airfoil.

Acknowledgments

The authors wish to gratefully acknowledge Yvan Tinel, Tinel Technologies for his efforts in the fabrication of the high-quality wind-tunnel models of the SA702x airfoils used in this work. Mark Drela is thanked for the XFOIL code used in this study.

References

[1]Donovan, J. F. and Selig, M. S., "Low Reynolds Number Airfoil Design and Wind Tunnel Testing at Princeton University," *Low Reynolds Number Aerodynamics*, edited by T. J. Mueller, Vol. 54 of *Lecture Notes in Engineering*, Springer-Verlag, New York, June 1989, pp. 39–57.

[2]Eppler, R., *Airfoil Design and Data*, Springer-Verlag, New York, 1990.

[3]Drela, M., "Low Reynolds-Number Airfoil Design for the M.I.T. Daedalus Prototype: A Case Study," *AIAA Journal*, Vol. 25, No. 8, August 1988, pp. 724–732.

[4]Selig, M. S., Gopalarathnam, A., Giguère, P., and Lyon, C. A., "Systematic Airfoil Design Studies at Low Reynolds Numbers," *Proceedings of the conference on Fixed, Flapping and Rotary Wing Vehicles at Very Low Reynolds Numbers*, edited by T. J. Mueller, June 2000, pp. 101–127, in review for a new volume of *Progress in Aeronautics and Astronautics* to be published by AIAA.

[5]Selig, M. S. and Maughmer, M. D., "A Multi-Point Inverse Airfoil Design Method Based on Conformal Mapping," *AIAA Journal*, Vol. 30, No. 5, May 1992, pp. 1162–1170.

[6]Selig, M. S. and Maughmer, M. D., "Generalized Multi-point Inverse Airfoil Design," *AIAA Journal*, Vol. 30, No. 11, November 1992, pp. 2618–2625.

[7]Drela, M., "XFOIL: An Analysis and Design System for Low Reynolds Number Airfoils," *Low Reynolds Number Aerodynamics*, edited by T. J. Mueller, Vol. 54 of *Lecture Notes in Engineering*, Springer-Verlag, New York, June 1989, pp. 1–12.

[8]Lyon, C. A., Selig, M. S., and Broeren, A. P., "Boundary Layer Trips on Airfoils at Low Reynolds Numbers," AIAA Paper 97-0511, January 1997.

[9]Lyon, C. A., Broeren, A. P., Giguère, P., Gopalarathnam, A., and Selig, M. S., *Summary of Low-Speed Airfoil Data, Vol. 3*, SoarTech Publications, Virginia Beach, Virginia, 1998.

[10]Selig, M. S., Donovan, J. F., and Fraser, D. B., *Airfoils at Low Speeds*, Soartech 8, SoarTech Publications, Virginia Beach, Virginia, 1989.

[11]Selig, M. S., Guglielmo, J. J., Broeren, A. P., and Giguère, P., *Summary of Low-Speed Airfoil Data, Vol. 1*, SoarTech Publications, Virginia Beach, Virginia, 1995.

[12]Selig, M. S., Lyon, C. A., Giguère, P., Ninham, C. N., and Guglielmo, J. J., *Summary of Low-Speed Airfoil Data, Vol. 2*, SoarTech Publications, Virginia Beach, Virginia, 1996.

Appendix A

In Appendix A, crossplots comparing the lift and drag data for the three airfoils at different trip locations and Reynolds numbers are presented.

Results with trip at 0.1*c*

Figures 17 and 18 compare the tripped performance of the three airfoils at Re=100,000 and 300,000 respectively, with the trip located at 0.1c on the upper surface.

Results with trip at 0.2*c*

Figures 19 and 20 compare the tripped performance of the three airfoils at Re=100,000 and 300,000 respectively, with the trip located at 0.2c on the upper surface.

Results with the trip located at 0.3*c*

Figures 21 and 22 compare the tripped performance of the three airfoils at Re=100,000 and 300,000 respectively, with the trip located at 0.3c on the upper surface.

Results with the trip located at 0.4*c*

Figures 23 and 24 compare the tripped performance of the three airfoils at Re=100,000 and 300,000 respectively. In each of these cases, the trip has been located at 0.4c on the upper surface.

Appendix B

In Appendix B, lift and drag data for each airfoil are compared for different trip locations and different Reynolds numbers.

Results for the SA7024

Figures. 25 and 26 present the lift and drag data for the SA7024 at a Reynolds number of 100,000 and 300,000 respectively for fie conditions: clean, trip located at 0.1c, trip located at 0.2c, trip located at 0.3c, and trip located at 0.4c.

Results for the SA7025

Figures. 27 and 28 present the lift and drag data for the SA7025 at a Reynolds number of 100,000 and 300,000 respectively for fie conditions: clean, trip located at 0.1c, trip located at 0.2c, trip located at 0.3c, and trip located at 0.4c.

Results for the SA7026

Figures. 29 and 30 present the lift and drag data for the SA7026 at a Reynolds number of 100,000 and 300,000 respectively for fie conditions: clean, trip located at 0.1c, trip located at 0.2c, trip located at 0.3c, and trip located at 0.4c.

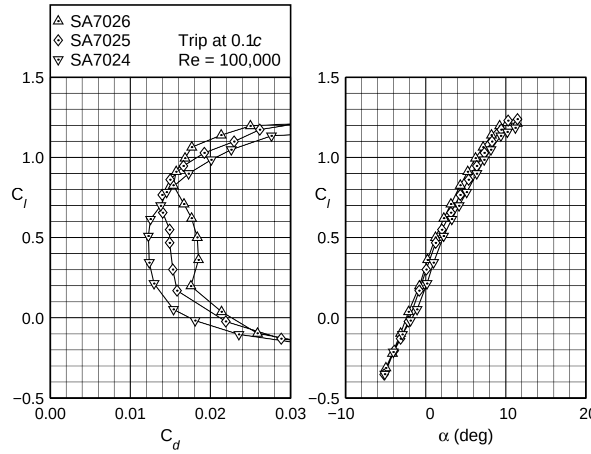

Fig. 17 Drag polars with trip at 0.1*c* for Re = 100,000.

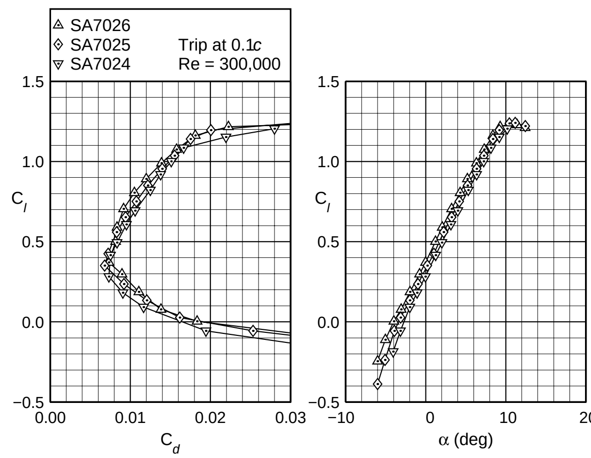

Fig. 18 Drag polars with trip at 0.1*c* for Re = 300,000.

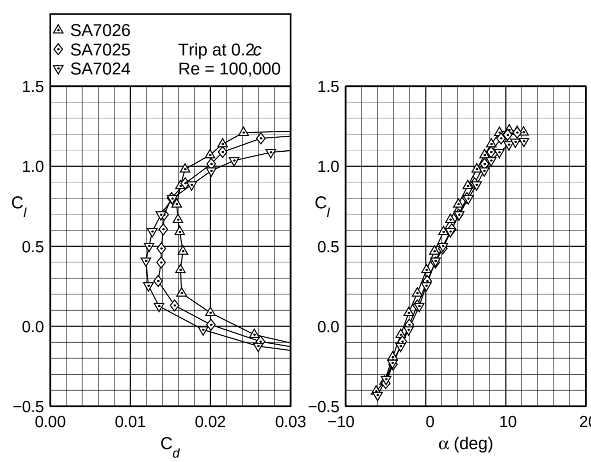

Fig. 19 Drag polars with trip at 0.2*c* for Re = 100,000.

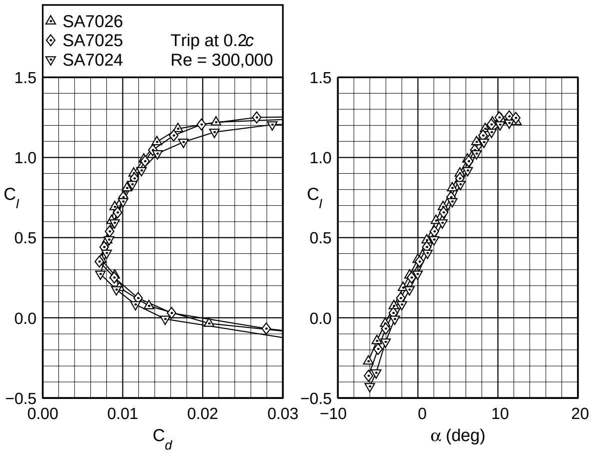

Fig. 20 Drag polars with trip at 0.2c for Re = 300,000.

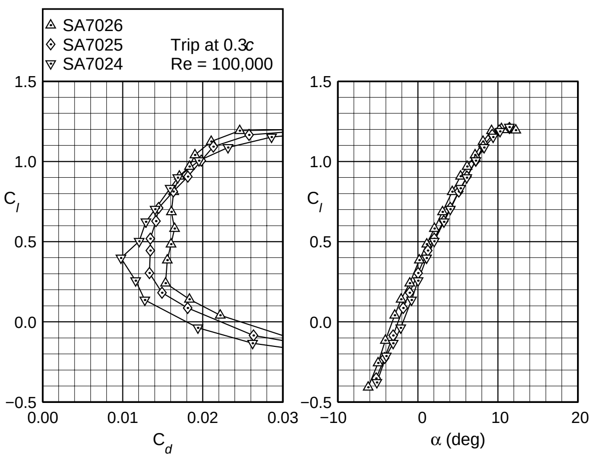

Fig. 21 Drag polars with trip at 0.3c for Re = 100,000.

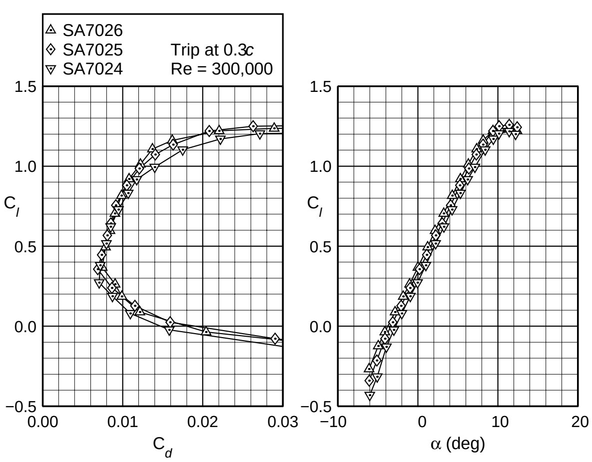

Fig. 22 Drag polars with trip at 0.3c for Re = 300,000.

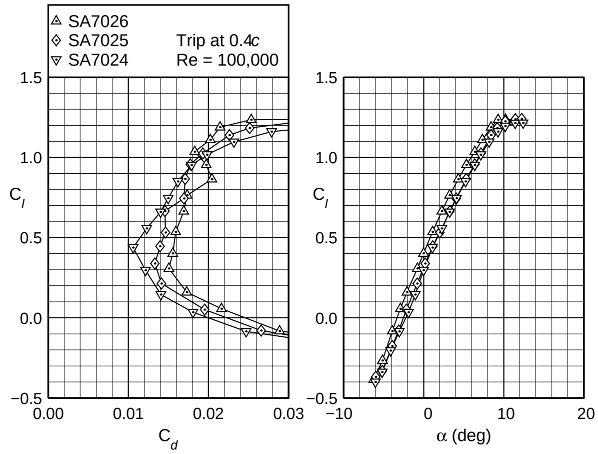

Fig. 23 Drag polars with trip at 0.4c for Re = 100,000.

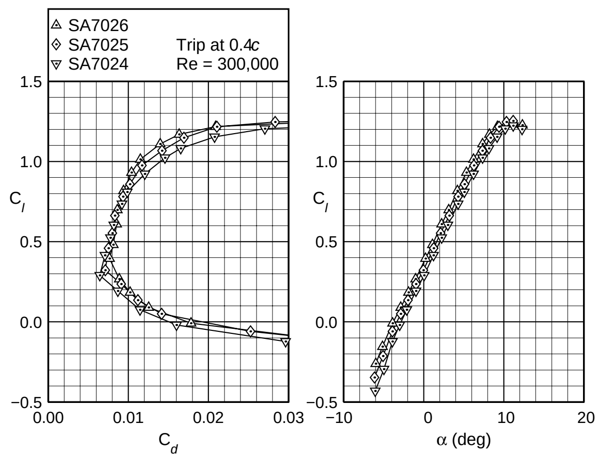

Fig. 24 Drag polars with trip at 0.4c for Re = 300,000.

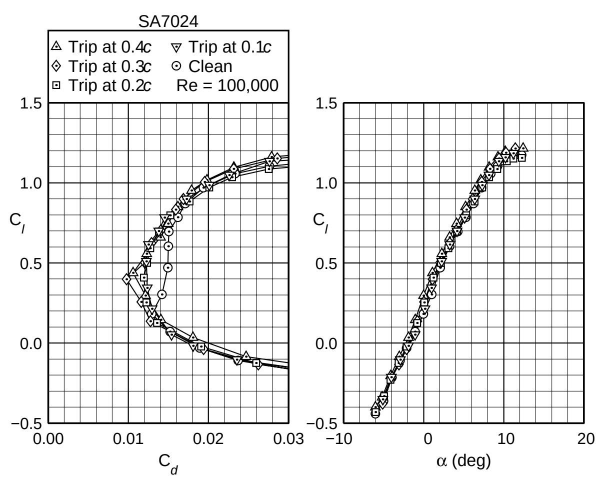

Fig. 25 Drag polars for the SA7024 at Re = 100,000.

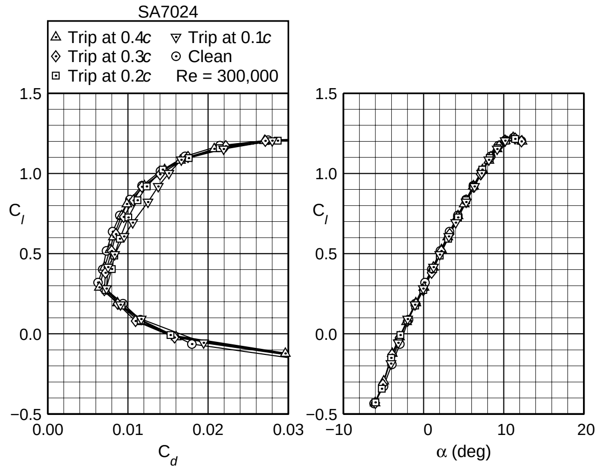

Fig. 26 Drag polars for the SA7024 at Re = 300,000.

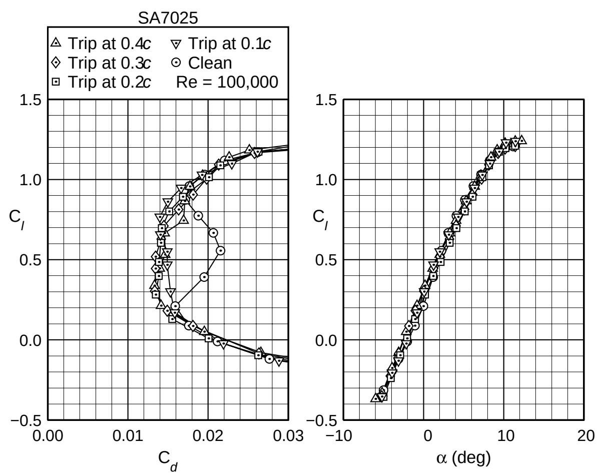

Fig. 27 Drag polars for the SA7025 at Re = 100,000.

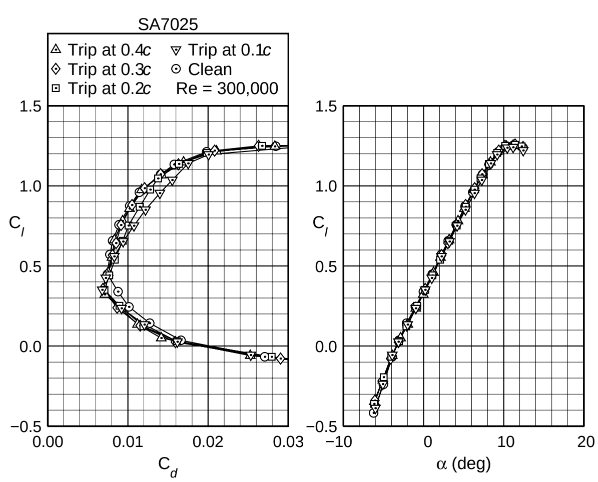

Fig. 28 Drag polars for the SA7025 at Re = 300,000.

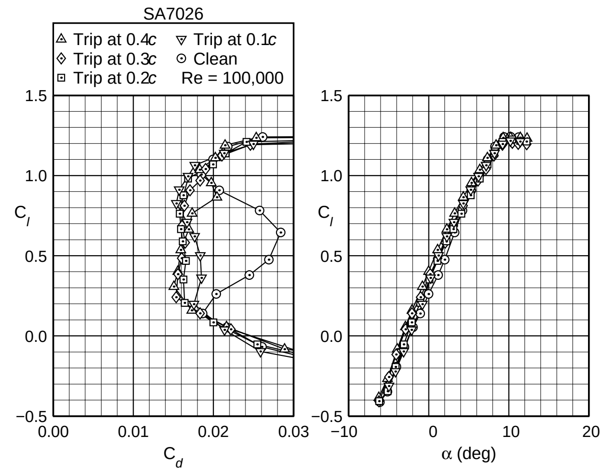

Fig. 29 Drag polars for the SA7026 at Re = 100,000.

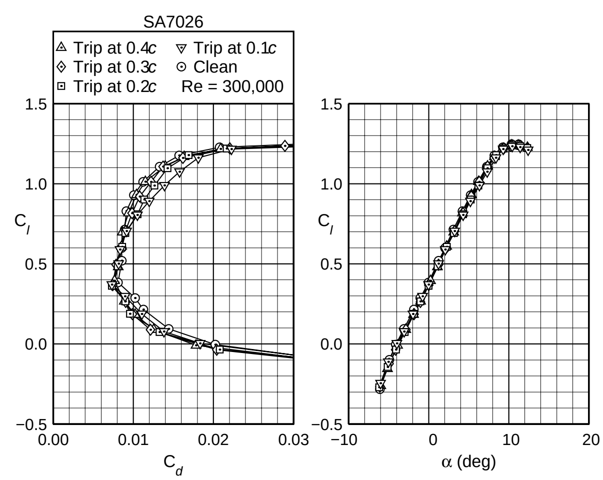

Fig. 30 Drag polars for the SA7026 at Re = 300,000.